applied sciences

MDPI

Article

Adsorption of Nitrate by a Novel Polyacrylic Anion Exchange Resin from Water with Dissolved Organic Matters: Batch and Column Study

Yue Sun [1,*], Weisheng Zheng [1], Xinchun Ding [2] and Rajendra Prasad Singh [1]

1 School of Civil Engineering, Southeast University, Nanjing 210096, China
2 Nanjing University & Yancheng Academy of Environmental Protection Technology and Engineering, Yancheng 224051, China
* Correspondence: sycyseu@163.com; Tel.: +86-25-83790750

Received: 6 July 2019; Accepted: 29 July 2019; Published: 30 July 2019

Featured Application: The novelty of this work is that the prepared resin AEE-3 has a potential application in the removal of nitrate from real secondary treated wastewater containing dissolved organic matters.

Abstract: A novel anion exchange resin AEE-3 was synthesized by N-alkylation of a weakly basic polyacrylic anion exchanger D311 with 1-bromopropane to effectively remove nitrate (NO_3^--N) from aqueous solution. The related finding revealed that its adsorption isotherm obeyed the Langmuir model well, and the second-order model was more validated for the NO_3^--N adsorption kinetics study. Compared to commercially-available polystyrene-based nitrate specialty resin Purolite A 520E (A520E), AEE-3 resin has a higher adsorbed amount and better regeneration performance toward NO_3^--N in the existence of dissolved organic matter (DOM) using static and dynamic methods. Notably, a real secondary treated wastewater (STWW) obtained from a local municipal wastewater treatment plant was also assessed for NO_3^--N removal in fixed-bed columns. Observations from this study indicated that AEE-3 could effectively remove NO_3^--N from contaminated surface water.

Keywords: nitrate; dissolved organic matter; ion exchange; selectivity

1. Introduction

With the rapid development of industry and agriculture, excessively-used nutrients such as nitrogen (N) and phosphorous (P) in crop production have been infiltrated into rivers, lakes and ponds, leading to the eutrophication of aquatic systems [1,2]. Nowadays, nitrate (NO_3^--N) pollution in surface and ground water is a severe environmental problem due to its carcinogenicity, toxicity and potential hazards to human health and livestock. Therefore, the World Health Organization (WHO) set the NO_3^--N concentration limit of 50 mg/L, whereas the U.S. Environmental protection Agency (U.S. EPA) allows 10 mg/L in drinking water [3,4].

Current approaches like reverse osmosis, electrodialysis, biological denitrification, adsorption and ion exchange have been utilized to treat NO_3^--N polluted water [5,6]. In consideration of the merits of ion exchange, such as high efficiency, acceptable regeneration and cost-effective preparation, anion exchange resins (AERs) have been employed to adsorb NO_3^--N from contaminated water [7–9]. On the basis of their chemical structure, commercial AERs are normally categorized into two skeletons, namely, polystyrene and polyacrylic. Polystyrene AERs have been used to effectively adsorb NO_3^--N from ground water in the past decade [10,11]. However, high concentrations of dissolved organic matters (DOMs) always exist in surface water, including secondary treated wastewater (STWW),

and can engender a strong affinity for resins via electrostatic attraction, hydrophobic interaction and so on [12–14]. Hence, AERs are more sensitive to fouling with DOMs, which would compete with NO_3^--N for the active sites and cause the decrease in NO_3^--N adsorption. More seriously, coexisting DOM could lead to an irreversible fixation to anion exchangers. Polyacrylic AERs with hydrophilic structures reveal a stronger resistance to organic fouling performance than polystyrene AERs [15]. Moreover, acrylic-based resins possess unique physiochemical properties, rapid adsorption rates and high ion-exchange capacities [16,17]. Accordingly, polyacrylic AERs could serve as a promising absorbent to effectively remove NO_3^--N from polluted water in the presence of DOMs. Nevertheless, few works have shown the feasibility of polyacrylic resins for NO_3^--N removal in real STWW containing NO_3^--N at high levels.

However, competitive anions such as chloride (Cl^-) or sulfate (SO_4^{2-}) exist widely in water, which can weaken NO_3^--N uptake efficacy of AERs [18]. To circumvent this limitation, studies have been devoted to preparing a novel anion exchanger with prominent selectivity toward NO_3^--N. The long alkyl chain addition at the exchange sites of resins could be of great benefit for the preferable selectivity toward monovalent anions because of its steric hindrance and hydrophobic effect [19,20]. Hence, it is intriguing for us to modify the weakly basic resin by introducing long alkyl groups around the active amine groups, which can easily form strongly basic functional groups (quaternary ammonium) which interact with NO_3^--N through strong electrostatic attraction.

Herein, a weakly basic polyacrylic anion exchanger D311 was modified with 1-bromopropane (C_3H_7Br) to prepare a strongly basic anion exchanger AEE-3 with high efficiency and brilliant selectivity for NO_3^--N uptake. The adsorption kinetics, isotherms, influence of pH value and competitive anions were investigated. In addition, commercial nitrate-selective polystyrene resin Purolite A 520E (A520E) was chosen to make a comparison with AEE-3 in both batch and fixed-bed column experiments, further demonstrating that AEE-3 is more resistant to fouling by DOMs (humic acid, tannic acid and sodium dodecyl benzene sulfonate). Also, a dynamic experiment was studied to evaluate the adsorption performance of AEE-3 toward NO_3^--N in real STWW.

2. Materials and Methods

2.1. Material

A commercially-available weakly basic anion exchanger D311 and strongly basic anion exchanger Purolite A 520E (A520E) were obtained from Huizhu Resin Co., Ltd. (Shanghai, China) and Purolite Co., Ltd. (Huzhou, China), respectively. Tannic acid (TA), humic acid (HA) and sodium dodecyl benzene sulfonate (SDBS) were purchased from Sinopharm Chemical Reagent Company (Shanghai, China). Other chemicals in this work were of analytical reagent acquired from Nanjing Chemical Reagent Co., Ltd. (Nanjing, China). STWW samples with a high NO_3^--N concentration were obtained from a local municipal wastewater treatment plant in Nanjing, China.

2.2. Preparation and Characterization of AEE-3

D311 resin was firstly rinsed successively with 1 mol/L HCl and 1 mol/L NaOH in turn to remove impurities, and then washed with deionized water until neutral. Finally, resin was washed by ethyl alcohol and then dried at 323 K for 8 h.

The synthesis method of AEE-3 is the following (Scheme 1): 10 g of dried D311 resin was swollen in 100 mL of acetonitrile for 2 h. Afterwards, 20 mmol of KI and 20 mmol C_3H_7Br were added separately and the mixture maintained with stirring at 333 K for 48 h. After alkylation, the obtained resin beads were rinsed successively with dilute HCl, distilled water and dilute NaOH to attain a neutral pH. Finally, the product was extracted with anhydrous ethanol and dried at 323 K for 8 h. The obtained resin AEE-3 was characterized by Fourier transform infrared spectrometer (Nicolet 5700, Madison, USA) and N_2 adsorption analysis (ASAP-2010C, Micromeritics, Norcross, GA, USA).

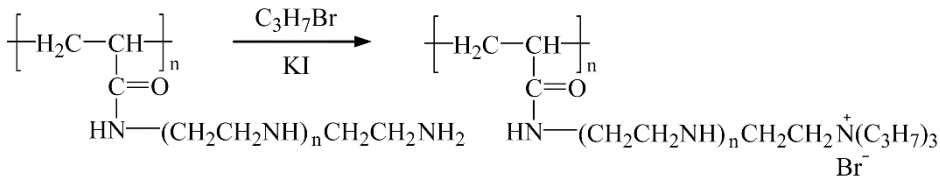

Scheme 1. The alkylation reaction of C_3H_7Br onto D311 resin.

2.3. Batch Adsorption Experiments

Isothermal adsorption experiments of NO_3^--N on adsorbents were performed when 0.05 g resin was introduced to each 150 mL conical flasks containing 50 mL of NO_3^--N in solution (10 to 60 mg/L concentration). To investigate the adsorption kinetics, 0.2 g resin was immersed into 200 mL NO_3^--N solution with the initial concentration of 60 mg/L, and samples were withdrawn at different time intervals. The pH (4.0–10.0) with 50 mg/L NO_3^--N solution in the presence of Cl^- (200 mg/L) was adjusted using 0.1 mol/L HCl or 0.1 mol/L NaOH solution, respectively, as required. A competing anion (SO_4^{2-} or Cl^-) was added to the NO_3^--N solution to study the effect of negative ions on adsorption capacities. The static tests of D311 and AEE-3 were conducted in a bi-solute system (HA/NO_3^-, SDBS/NO_3^- or TA/NO_3^-) for four adsorption-desorption cycles. Analyses of NO_3^--N were obtained by measuring the UV1800 spectrophotometer at a wavelength of 220 nm. The adsorption amount Q_e (mg/g) was calculated using Equation (1):

$$Q_e = \frac{(C_0 - C_e)V}{W} \tag{1}$$

where C_0 and C_e are the initial and equilibrium concentrations (mg/L) of NO_3^--N, V is the volume of solution (L) and W represents the weight of dry resin (g).

2.4. Column Adsorption and Desorption

The experiments were carried out using a glass column (Φ18 × 200 mm) with 5 mL of dry fresh resin and a peristaltic pump to ensure the constant flow rate under 298 K. The initial concentration of NO_3^--N was 20 mg/L, containing 1 mg/L TA, 1 mg/L HA and 2 mg/L SDBS. The superficial liquid velocity (SLV) was 30 bed volume per hour (BV/h), and the breakthrough curve was obtained by analysis of different time intervals of the effluent. After adsorption, the elution of NO_3^--N from the resin was performed using 0.6 mol/L NaCl solution. The adsorption–desorption cycle was repeated three times to evaluate the regeneration efficiency of resins. The desorption rate (D) of NO_3^--N was defined by Equation (2):

$$D(\%) = \frac{C_d}{C_a} \times 100 \tag{2}$$

where C_a is the amount of NO_3^--N adsorbed on resins and C_d is the amount of NO_3^--N desorbed from resins by NaCl solution.

3. Results and Discussion

3.1. Characterization

The adsorption-desorption isotherms and the pore size distribution curve of D311 and AEE-3 are displayed in Figure 1. The isotherm plot of two resins can be considered type IV with a hysteresis loop in the relative pressure range of 0.8–1.0, hinting at the existence of both mesopores and macropores in these resins. Table 1 lists the essential properties of D311 and AEE-3.

The FT-IR spectra of D311 and AEE-3 samples are shown in Figure 2. Notably, two bands with peaks at 1366 cm^{-1} and 2930 cm^{-1} are ascribed to asymmetric bands of the alkyl groups (–CH_2–and-CH_3), and the peak at 1478 cm^{-1} is assigned to C–N group. The appearance of a new band at 1407 cm^{-1}

is associated with $–CH_2–of–CH_2–N^+R_3$ group [7]. On the other side, the fact that the strong base ion-exchange capacity of the resin increased from 0 to 3.42 mmol/g implied that propyl groups were successfully introduced onto the primary amine after alkylation. These observations proved AEE-3 had been synthesized successfully.

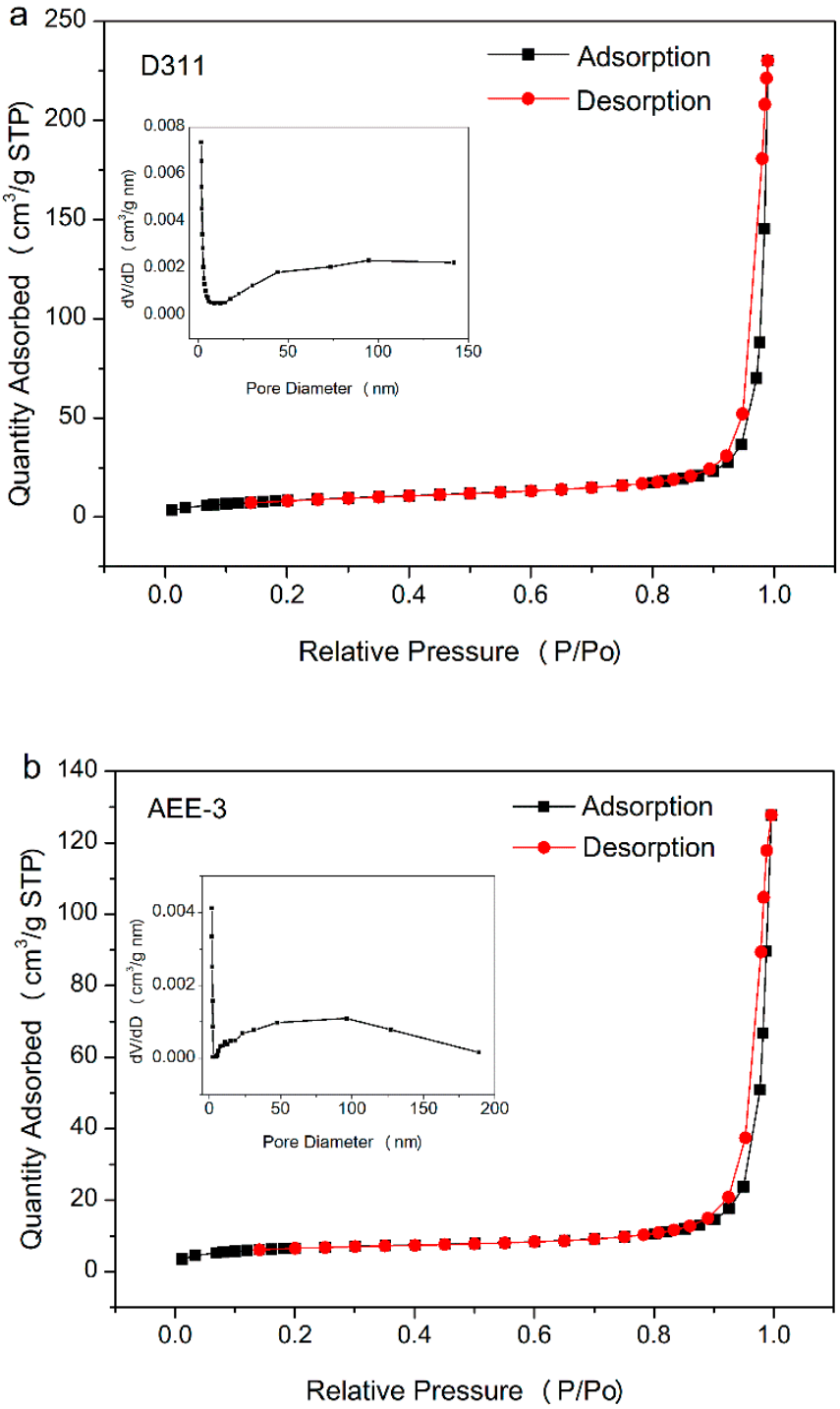

Figure 1. Nitrogen adsorption–desorption isotherms of D311 (**a**) and AEE-3 (**b**) with inset showing the corresponding pore size distribution.

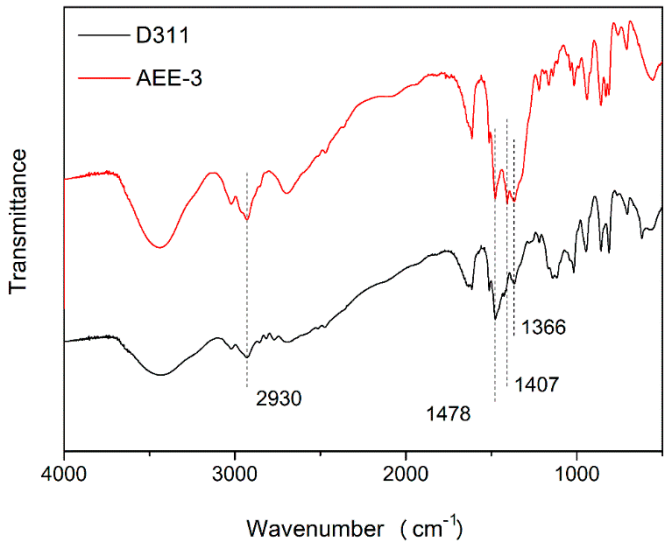

Figure 2. FT-IR spectra of D311 and AEE-3.

Table 1. Physicochemical properties of two resins.

Resin	Strong Base Ion-Exchange Capacity (mmol/g Dry Resin)	Average Pore Diameter [a] (nm)	BET Surface Area (m^2/g)	Pore Volume (cm^3/g)
D311	0	40.92	31.88	0.36
AEE-3	3.42	47.44	23.46	0.20

[a] BJH Desorption average pore diameter.

3.2. Adsorption Kinetics

Figure 3 describes the effect of contact time on NO_3^--N uptake by AEE-3 and A520E at 298 K, and all the data were simulated using two commonly used kinetic models [21,22]:

$$\text{Pseudo} - \text{first} - \text{order}: \; Q_t = Q_e(1 - e^{-k_1 t}) \tag{3}$$

$$\text{Pseudo} - \text{second} - \text{order}: \; Q_t = \frac{k_2 Q_e^2 t}{1 + k_2 Q_e t} \tag{4}$$

The initial adsorption rate was calculated by Equation (5):

$$h_0 = k_2 Q_e^2 \tag{5}$$

where Q_e (mg/g) is the equilibrium adsorption capacity of NO_3^--N, and Q_t (mg/g) refers to the amounts of NO_3^--N in resins at time t (min). k_1 (1/min) and k_2 (g/(mg·min)) represent the rate constants for the pseudo-first- and pseudo-second-order kinetic models, respectively. h_0 is the initial adsorption rate (mg/(g·min)). The kinetic parameters, together with the coefficient of determination (R^2), are listed in Table 2. It is evident that the adsorption behavior of NO_3^--N onto both resins was preferable to fit the pseudo-second-order based on the R^2 values. Obviously, AEE-3 exhibited a greater capacity for NO_3^--N than A520E, illustrating that the introduction of alkyl chains would form quaternary ammonium groups which can easily interact with NO_3^--N via electrostatic attraction. Finally, a larger h_0 value of AEE-3 was obtained, and the difference in the adsorption rate is related to the difference of the resin matrix.

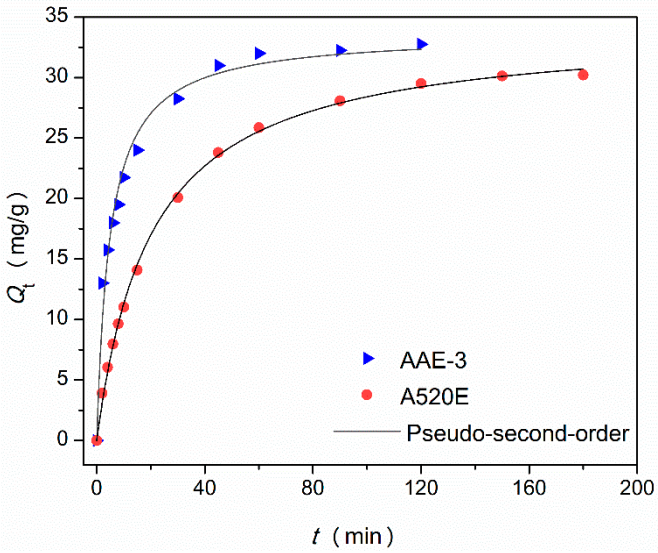

Figure 3. Adsorption kinetics of NO_3^--N onto two resins at 298 K.

Table 2. Kinetic parameters of NO_3^--N adsorption by two resins.

Resin	$Q_{e,\,exp}$ (mg/g)	Pseudo-First-Order			Pseudo-Second-Order			
		Q_e (mg/g)	k_1 (1/min)	R^2	Q_e (mg/g)	$10^3 k_2$ (g/(mg·min))	R^2	h_0 (mg/(g·min))
AEE-3	32.75	30.85	0.327	0.9371	33.66	6.06	0.9819	7.13
A520E	30.22	29.19	0.100	0.9897	30.14	1.45	0.9987	1.16

3.3. *Effect of Coexisting Anions*

In general, some coexisting anions in water would strongly compete with NO_3^--N to occupy active sites via electrostatic interaction. Thus, the selective absorption of resin is of vital importance in evaluating the practical application, as well as in considering the absorption performance. A520E is known for its good selectivity toward NO_3^--N, and its adsorption capacities are still relatively high in the present of Cl^- or SO_4^{2-} [20]. As displayed in Figure 4, a slightly higher adsorption amount of AEE-3 was detected compared to A520E with an identical addition of anions. The phenomena may be rationalized by the fact that the long alkyl chain on AEE-3 is conducive to the adsorption selectivity for NO_3^--N with lower hydration energy than Cl^- or SO_4^{2-}.

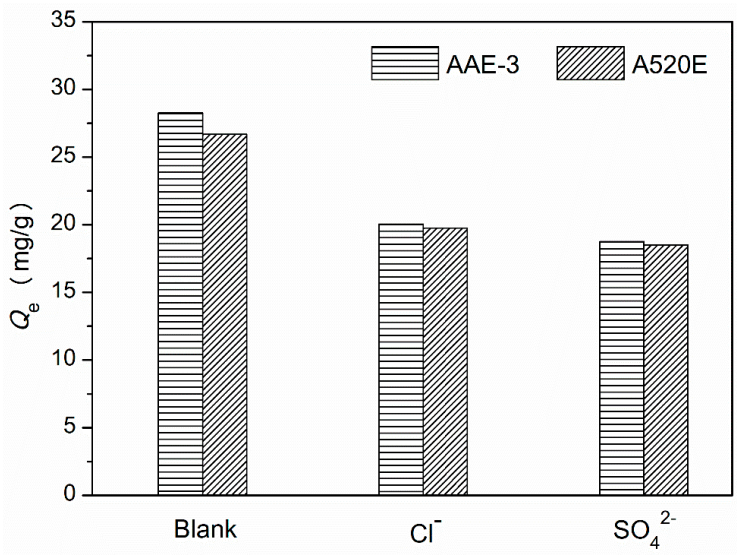

Figure 4. Effect of competitive anions Cl^- and SO_4^{2-} on NO_3^--N removal by two resins.

3.4. Effect of pH

The primary mechanism for NO_3^--N uptake onto a strongly basic anion exchanger can be explained by electrostatic interaction or columbic force [23]. Figure 5 displays the influence of solution pH varying from 4.0 and 10.0; the adsorption capacity of NO_3^--N on AEE-3 was in the range of 25.5 to 26.0 mg/g under a Cl^- concentration of 200 mg/L. It shows a considerable amount of NO_3^--N uptake independent of the pH for the strongly basic anion exchanger. It may be concluded that the quaternary tripropylamine groups of AEE-3 could remain stable, thereby causing steady adsorption activity for NO_3^--N under both acidic and alkaline conditions [24].

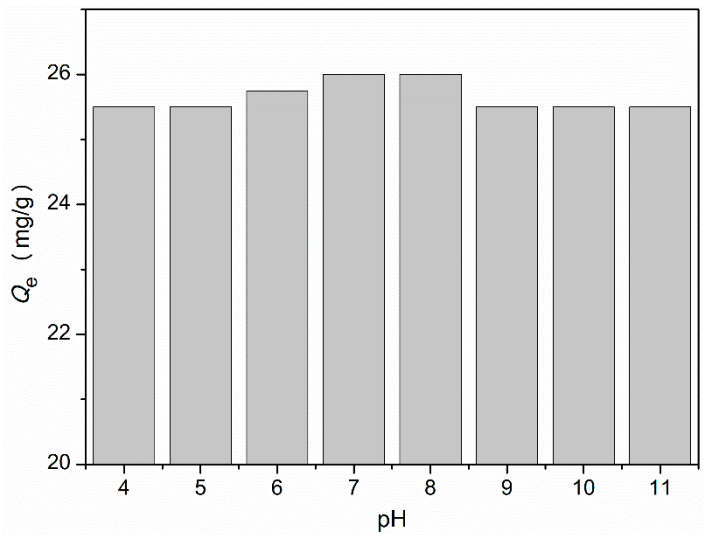

Figure 5. Effect of pH on NO_3^--N removal by AEE-3.

3.5. Adsorption Isotherms

The isotherms of NO_3^--N adsorption by AEE-3 are displayed in Figure 6. The experimental data were fitted by both Langmuir and Freundlich equations which are represented as follows [25,26]:

$$Q_e = \frac{Q_m K_L C_e}{1 + K_L C_e} \quad (6)$$

$$Q_e = K_F C_e^{1/n} \quad (7)$$

where C_e (mg/L) is the concentration at equilibrium state, Q_e (mg/g) is the adsorption capacity at equilibrium state, Q_m (mg/g) is the maximum adsorption capacity, K_L is the Langmuir constant and K_F and n are the Freundlich constants. The R^2 of the isothermal fit are presented in Table 3. In view of the R^2 values, the equilibrium adsorption of NO_3^--N onto AEE-3 was better described by the Langmuir isotherm, which coincided with the prevalent ion-exchange mechanism [7,23]. Moreover, the Q_m values of AEE-3 dropped with the increase of temperature, revealing that the NO_3^--N adsorption by the resin was an exothermic process, and therefore, reducing the temperature benefited NO_3^--N uptake.

The maximum NO_3^--N adsorption amount of AEE-3, as evaluated according to the Langmuir model, was compared with other materials including chitosan, activated carbon and commercial anion exchange resins (A520E and D201), etc. As shown in Table 4, the Q_m of AEE-3 for NO_3^--N uptake was higher than that of these commercially available materials, signifying that the novel anion exchange resin can act as a potential material for the technological application of NO_3^--N removal from water.

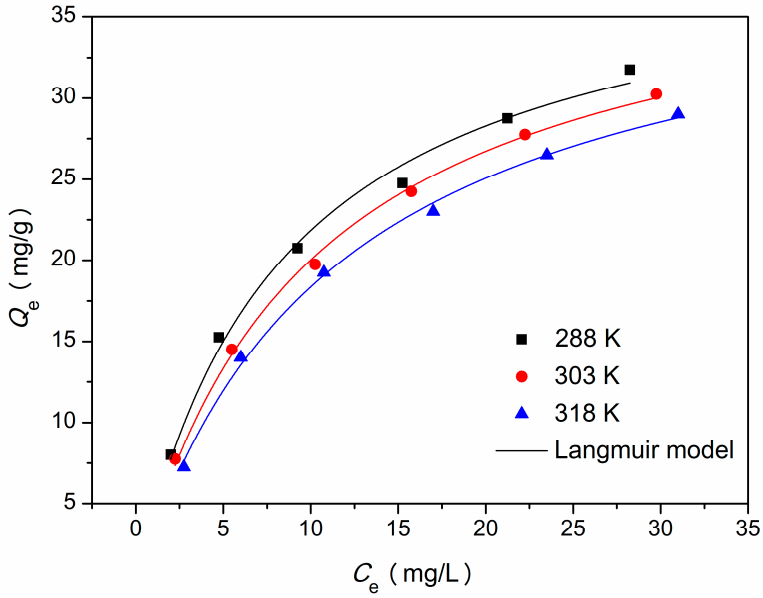

Figure 6. Equilibrium isotherm for NO_3^--N adsorbed using AEE-3.

Table 3. Isotherm parameters for NO_3^--N adsorption at 288, 303, and 318 K.

T (K)	Langmuir Model			Freundlich Model		
	K_L	Q_m (mg/g)	R^2	K_F	n	R^2
288	0.12	40.32	0.9915	7.18	2.21	0.9816
303	0.10	40.00	0.9977	6.39	2.13	0.9810
318	0.09	39.45	0.9973	5.66	2.06	0.9721

Table 4. Comparison of NO_3^--N maximum adsorption capacity (Q_m) by different materials.

Samples	Q_m (mg/g)	Reference
Chitosan/PVA	35.00	[27]
Cationic polymer-modified granular activated carbon (CPMG)	27.56	[28]
Modified commercial activated carbon	21.51	[29]
Magnetic anion-exchange resin MD217	30.40	[30]
A520E	36.15	[31]
D201	38.46	[31]
AEE-3	40.32	This study

3.6. Effect of DOMs on Static Adsorption and Desorption

Figure 7 shows the adsorption amounts of NO_3^--N using AEE-3 and A520E in a bi-solute system (HA/NO_3^-, SDBS/NO_3^- or TA/NO_3^-) for four adsorption-desorption cycles. It was seen that the adsorption capacities of A520E for NO_3^--N distinctly declined over the four cycles. DOMs can occupy more active sites through hydrophobic and electrostatic interactions on the A520E resin with a polystyrene matrix [12]. By contrast, AEE-3 exhibited greater NO_3^--N adsorption in bi-solute systems, and the reduction of NO_3^--N uptake was slight with increasing the number of adsorption-desorption cycles. This result validated the hypothesis that AEE-3 has a strong resistance to interferential organics due to its hydrophilic matrix. Besides, over 94% of the adsorbed NO_3^--N on AEE-3 was desorbed, while the desorption rates of A520E in the presence of organic matters declined gradually with the number of adsorption-desorption cycle (Figure 8). In addition, Figure 9 presents the desorption rates of DOMs regenerated by a NaCl solution, and the low values for A520E resin can be attributed to the strong affinity between the polystyrene matrix and the hydrophobic organics, causing the DOMs to not be removed fully by regeneration. Hence, these results demonstrate an improved performance on adsorption/regeneration of AEE-3 compared to A520E.

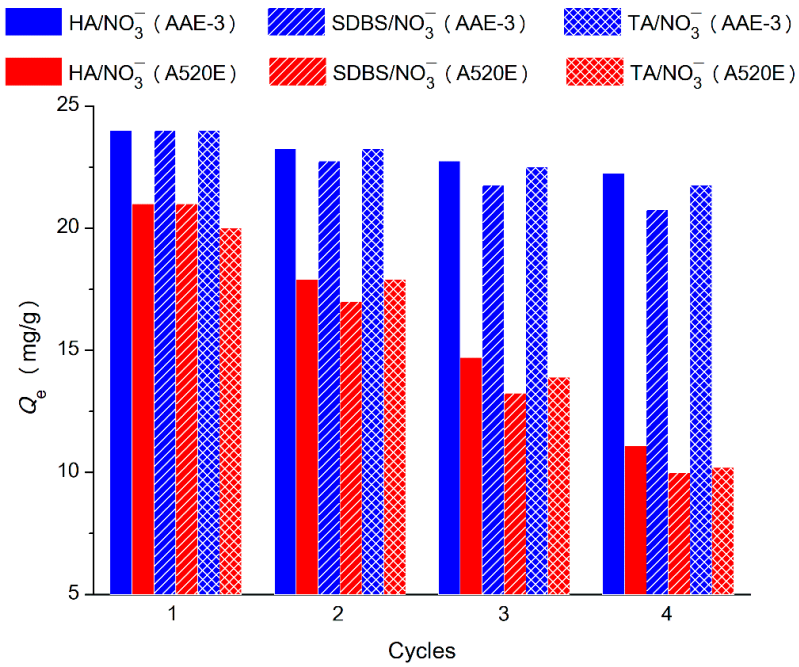

Figure 7. Effect of different DOMs (HA, TA or SDBS) on NO_3^--N removal by AEE-3 and A520E.

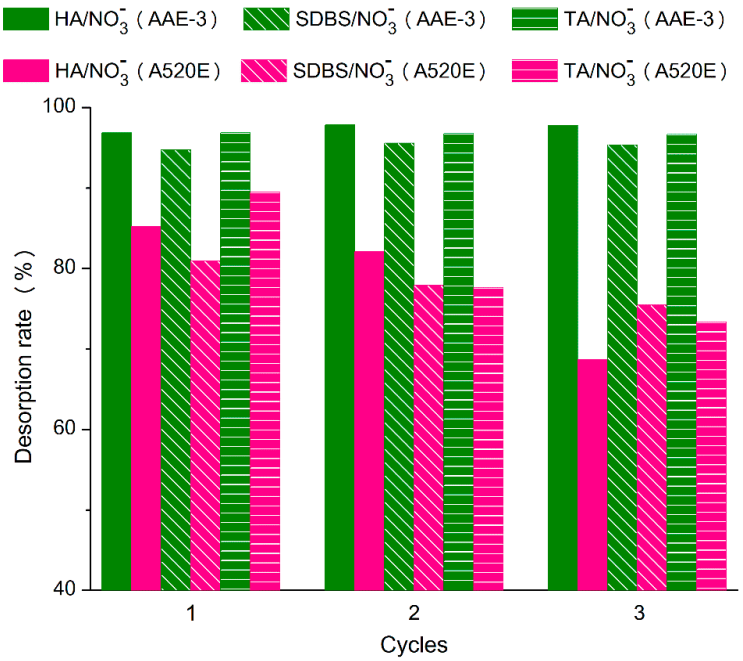

Figure 8. Desorption rate of NO_3^--N in the presence of DOMs.

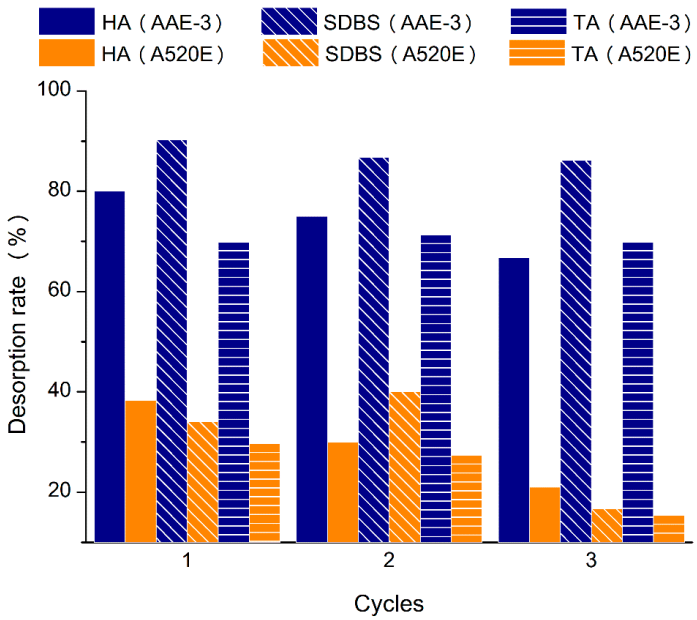

Figure 9. Desorption rates of different DOMs (HA, TA or SDBS) by AEE-3 and A520E.

3.7. Effect of DOMs on Column Mode Experiments

It is imperative to test the utilization efficiency of adsorbents in a dynamic fixed-bed experiment related to real operating systems [32]. The influence of three organics on NO_3^--N adsorption was studied using an influent with constant NO_3^--N concentration of 20 mg/L in the presence of HA, TA and SDBS. As can be seen in Figure 10, the breakthrough curves (Run 2 and Run 3) for NO_3^--N adsorption onto AEE-3 have a close coincidence with the original breakthrough curve (Run 1). Nevertheless, a large separation between the three breakthrough curves was observed for NO_3^--N adsorption onto A520E, which is indicative of a limited reusability of A520E towards NO_3^--N solution containing DOMs.

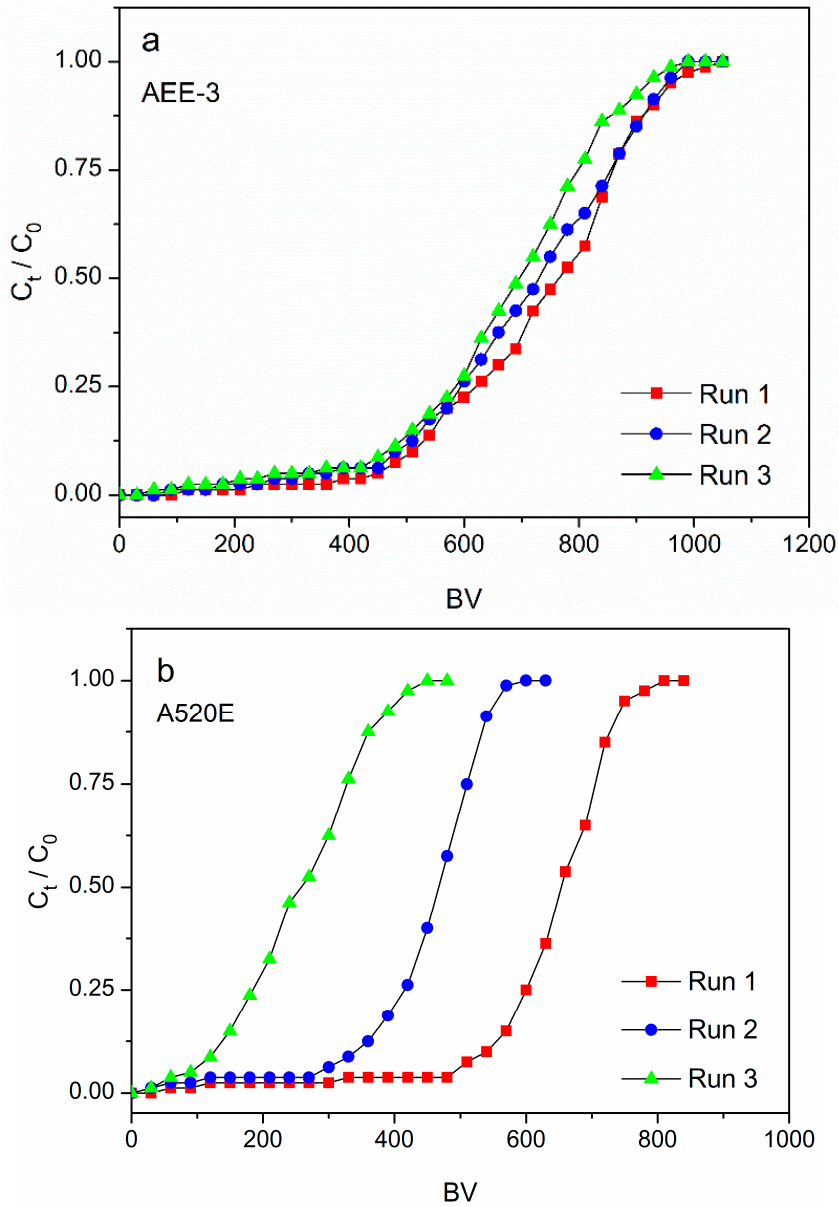

Figure 10. NO_3^--N breakthrough curves of AEE-3 (**a**) and A520E (**b**) for presence of HA, TA and SDBS.

3.8. Assessments of Practical Application

Conventional heterotrophic denitrification techniques are severely restricted by the low C/N ratio of wastewater, thereby causing the high NO_3^--N content in STWW [33,34]. To further assess the practical application of AEE-3, the dynamic column test of NO_3^--N uptake onto AEE-3 was performed using a real STWW effluent which was collected from a local sewage treatment plant, containing the following quality parameters: pH, 6.54; NO_3^--N, 20 mg/L; COD, 39 mg/L; TDS, 436 mg/L. The breakthrough curves of AEE-3 are shown in Figure 11. An inconspicuous deviation between Run 1 and Run 3 breakthrough curves was found, further confirming its potential application in the removal of NO_3^--N from real STWW effluent.

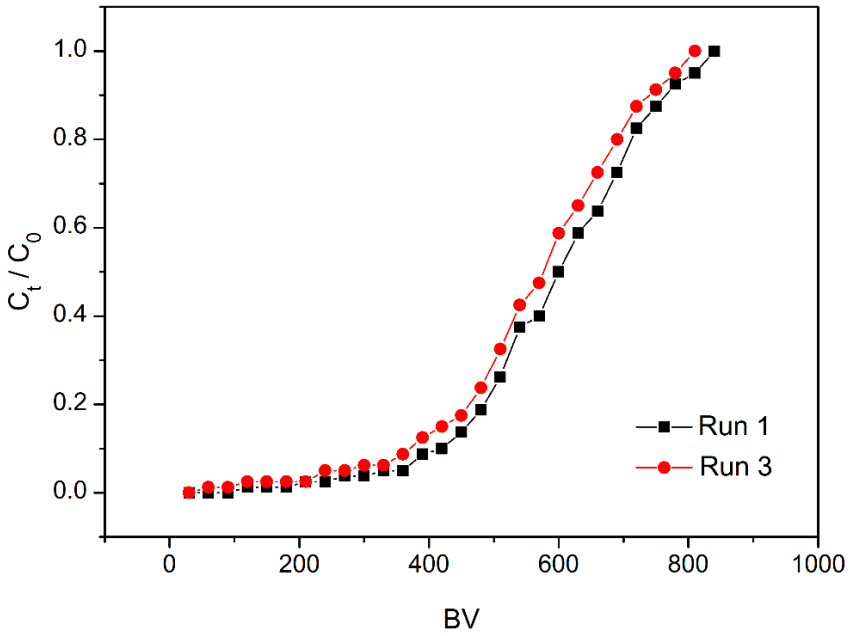

Figure 11. Breakthrough curves of NO_3^--N adsorbed on AEE-3 in real STWW.

4. Conclusions

The strong base polyacrylic AER AEE-3 could be developed and utilized to absorb NO_3^--N selectively from aqueous solutions. Batch adsorption studies exhibited that a pseudo-second-order model was appropriate for depicting the kinetic process, and that the best fit for the isotherms data was Langmuir model. In addition, AEE-3 displayed a greater adsorption capacity and better regeneration capability for NO_3^--N uptake than the commonly-used, nitrate-selective AER A520E in the presence of interferential DOMs. Notably, the effective adsorption of NO_3^--N in real STWW by AEE-3 packed in fixed-bed columns revealed its promising potential in the removal of NO_3^--N from actual complex wastewater.

Author Contributions: Conceptualization, Y.S.; Formal analysis, Y.S.; Funding acquisition, Y.S.; Resources, X.D.; Visualization, W.Z.; Writing—original draft, Y.S.; Writing—review & editing, W.Z. and R.P.S.

Funding: This research was funded by National Natural Science Foundation of China (No. 51578131) and Open Foundation of Institute of Water Environmental Engineering, Jiangsu Industrial Technology Research Institute, Yancheng (NDYCKF201701). The APC was funded by Open Foundation of Institute of Water Environmental Engineering, Jiangsu Industrial Technology Research Institute, Yancheng (NDYCKF201701).

Acknowledgments: We thank the reviewers for their insightful comments and suggestions.

Conflicts of Interest: The authors declare no conflict of interest.

References

1. Chowdhury, R.B.; Moore, G.A.; Weatherley, A.J.; Arora, M. A novel substance flow analysis model for analysing multi-year phosphorus flow at the regional scale. *Sci. Total Environ.* **2016**, *572*, 1269–1280. [CrossRef] [PubMed]
2. Yang, Z.; Zhang, M.; Shi, X.; Kong, F.; Ma, R.; Yu, Y. Nutrient reduction magnifies the impact of extreme weather on cyanobacterial bloom formation in large shallow Lake Taihu. *Water Res.* **2016**, *103*, 302–310. [CrossRef] [PubMed]
3. Loganathan, P.; Vigneswaran, S.; Kandasamy, J. Enhanced removal of nitrate from water using surface modification of adsorbents—A review. *J. Environ. Manag.* **2013**, *131*, 363–374. [CrossRef] [PubMed]
4. Hafshejani, L.D.; Hooshmand, A.; Naseri, A.A.; Mohammadi, A.S.; Abbasi, F.; Bhatnagar, A. Removal of nitrate from aqueous solution by modified sugarcane bagasse biochar. *Ecol. Eng.* **2016**, *95*, 101–111. [CrossRef]

5. Kalaruban, M.; Loganathan, P.; Shim, W.; Kandasamy, J.; Ngo, H.; Vigneswaran, S. Enhanced removal of nitrate from water using amine-grafted agricultural wastes. *Sci. Total. Environ.* **2016**, *565*, 503–510. [CrossRef] [PubMed]
6. Epsztein, R.; Nir, O.; Lahav, O.; Green, M. Selective nitrate removal from groundwater using a hybrid nanofiltration–reverse osmosis filtration scheme. *Chem. Eng. J.* **2015**, *279*, 372–378. [CrossRef]
7. Song, H.; Zhou, Y.; Li, A.; Mueller, S. Selective removal of nitrate from water by a macroporous strong basic anion exchange resin. *Desalination* **2012**, *296*, 53–60. [CrossRef]
8. Bergquist, A.M.; Choe, J.K.; Strathmann, T.J.; Werth, C.J. Evaluation of a hybrid ion exchange-catalyst treatment technology for nitrate removal from drinking water. *Water Res.* **2016**, *96*, 177–187. [CrossRef]
9. Ebrahimi, S.; Roberts, D.J. Bioregeneration of single use nitrate selective ion-exchange resin enclosed in a membrane: Kinetics of desorption. *Sep. Purif. Technol.* **2015**, *146*, 268–275. [CrossRef]
10. Samatya, S.; Kabay, N.; Yüksel, Ü.; Arda, M.; Yüksel, M. Removal of nitrate from aqueous solution by nitrate selective ion exchange resins. *React. Funct. Polym.* **2006**, *66*, 1206–1214. [CrossRef]
11. Wu, Y.; Wang, Y.; Wang, J.; Xu, S.; Yu, L.; Philippe, C.; Wintgens, T. Nitrate removal from water by new polymeric adsorbent modified with amino and quaternary ammonium groups: Batch and column adsorption study. *J. Taiwan Inst. Chem. Eng.* **2016**, *66*, 191–199. [CrossRef]
12. Shuang, C.; Wang, J.; Li, H.; Li, A.; Zhou, Q. Effect of the chemical structure of anion exchange resin on the adsorption of humic acid: Behavior and mechanism. *J. Colloid Interface Sci.* **2015**, *437*, 163–169. [CrossRef] [PubMed]
13. Wang, Q.; Li, A.; Wang, J.; Shuang, C. Selection of magnetic anion exchange resins for the removal of dissolved organic and inorganic matters. *J. Environ. Sci.* **2012**, *24*, 1891–1899. [CrossRef]
14. Wang, J.; Zhou, Y.; Li, A.; Xu, L. Adsorption of humic acid by bi-functional resin JN-10 and the effect of alkali-earth metal ions on the adsorption. *J. Hazard. Mater.* **2010**, *176*, 1018–1026. [CrossRef] [PubMed]
15. Shuang, C.; Wang, M.; Zhou, Q.; Zhou, W.; Li, A. Enhanced adsorption and antifouling performance of anion-exchange resin by the effect of incorporated Fe_3O_4 for removing humic acid. *Water Res.* **2013**, *47*, 6406–6414. [CrossRef] [PubMed]
16. Wójcik, G.; Neagu, V.; Bunia, I. Sorption studies of chromium(VI) onto new ion exchanger with tertiary amine, quaternary ammonium and ketone groups. *J. Hazard. Mater.* **2011**, *190*, 544–552. [CrossRef] [PubMed]
17. Dan, Z.; Xiao, K.; Han, G.; Li, J.; Xu, F.; Jiang, L.; Duan, N. Evaluation of polyacrylic anion exchange resins on the removal of Cr(vi) from aqueous solutions. *RSC Adv.* **2016**, *6*, 5233–5239.
18. Hekmatzadeh, A.; Karimi-Jashani, A.; Talebbeydokhti, N.; Kløve, B. Modeling of nitrate removal for ion exchange resin in batch and fixed bed experiments. *Desalination* **2012**, *284*, 22–31. [CrossRef]
19. Wang, J.; Wang, Q.; Deng, Y.; Li, Y.; Chen, B.H.; Zhang, R. Modified polystyrene anion exchange resins with long chain alkyl groups to enhance the aldolization reaction selectivity. *Appl. Catal. A Gen.* **2013**, *452*, 57–63. [CrossRef]
20. Chauhan, K.; Kaur, J.; Singh, P.; Sharma, P.; Sharma, P.; Chauhan, G.S. An Efficient and Regenerable Quaternary Starch for Removal of Nitrate from Aqueous Solutions. *Ind. Eng. Chem. Res.* **2016**, *55*, 2507–2519. [CrossRef]
21. Wang, L. Application of activated carbon derived from waste bamboo culms for the adsorption of azo disperse dye: Kinetic, equilibrium and thermodynamic studies. *J. Environ. Manag.* **2012**, *102*, 79–87. [CrossRef] [PubMed]
22. Saki, H.; Alemayehu, E.; Schomburg, J.; Lennartz, B. Halloysite Nanotubes as Adsorptive Material for Phosphate Removal from Aqueous Solution. *Water* **2019**, *11*, 203. [CrossRef]
23. Li, Q.; Lu, X.; Shuang, C.; Qi, C.; Wang, G.; Li, A.; Song, H. Preferential adsorption of nitrate with different trialkylamine modified resins and their preliminary investigation for advanced treatment of municipal wastewater. *Chemosphere* **2019**, *223*, 39–47. [CrossRef] [PubMed]
24. Gu, B.; Ku, Y.K.; Jardine, P.M. Sorption and Binary Exchange of Nitrate, Sulfate, and Uranium on an Anion-Exchange Resin. *Environ. Sci. Technol.* **2004**, *38*, 3184–3188. [CrossRef] [PubMed]
25. Xu, X.; Bai, B.; Wang, H.; Suo, Y. Enhanced adsorptive removal of Safranine T from aqueous solutions by waste sea buckthorn branch powder modified with dopamine: Kinetics, equilibrium, and thermodynamics. *J. Phys. Chem. Solids* **2015**, *87*, 23–31. [CrossRef]
26. Wasielewski, S.; Rott, E.; Minke, R.; Steinmetz, H. Evaluation of Different Clinoptilolite Zeolites as Adsorbent for Ammonium Removal from Highly Concentrated Synthetic Wastewater. *Water* **2018**, *10*, 584. [CrossRef]

27. Rajeswari, A.; Amalraj, A.; Pius, A. Adsorption studies for the removal of nitrate using chitosan/PEG and chitosan/PVA polymer composites. *J. Water Process. Eng.* **2016**, *9*, 123–134. [CrossRef]
28. Cho, D.W.; Chon, C.M.; Kim, Y.; Jeon, B.H.; Schwartz, F.W.; Lee, E.S.; Song, H. Adsorption of nitrate and Cr(VI) by cationic polymer-modified granular activated carbon. *Chem. Eng. J.* **2011**, *175*, 298–305. [CrossRef]
29. Mazarji, M.; Aminzadeh, B.; Baghdadi, M.; Bhatnagar, A. Removal of nitrate from aqueous solution using modified granular activated carbon. *J. Mol. Liq.* **2017**, *233*, 139–148. [CrossRef]
30. Wang, B.; Song, H.; Wang, C.; Shuang, C.; Li, Q.; Li, A. Evaluation of nitrate removal properties of magnetic anion-exchange resins in water. *J. Chem. Technol. Biotechnol.* **2016**, *91*, 1306–1313. [CrossRef]
31. Song, H.O.; Yao, Z.J.; Wang, M.Q.; Wang, J.N.; Zhu, Z.L.; Li, A.M. Effect of dissolved organic matter on nitrate-nitrogen removal by anion exchange resin and kinetics studies. *J. Environ. Sci.* **2013**, *25*, 105–113. [CrossRef]
32. Xu, X.; Gao, B.; Zhao, Y.; Chen, S.; Tan, X.; Yue, Q.; Lin, J.; Wang, Y. Nitrate removal from aqueous solution by Arundo donax L. reed based anion exchange resin. *J. Hazard. Mater.* **2012**, *203*, 86–92. [CrossRef] [PubMed]
33. Yang, Y.; Chen, T.; Morrison, L.; Gerrity, S.; Collins, G.; Porca, E.; Li, R.; Zhan, X. Nanostructured pyrrhotite supports autotrophic denitrification for simultaneous nitrogen and phosphorus removal from secondary effluents. *Chem. Eng. J.* **2017**, *328*, 511–518. [CrossRef]
34. Kong, D.; Li, W.; Deng, Y.; Ruan, Y.; Chen, G.; Yu, J.; Lin, F. Denitrification-Potential Evaluation and Nitrate-Removal-Pathway Analysis of Aerobic Denitrifier Strain Marinobacter hydrocarbonoclasticus RAD-2. *Water* **2018**, *10*, 1298. [CrossRef]